WILEY Blackwell

the FEBS Journal

Volume 282 Number 15 August 2015 | ISSN 1742-464X www.febsjournal.org

Protein nanotubes

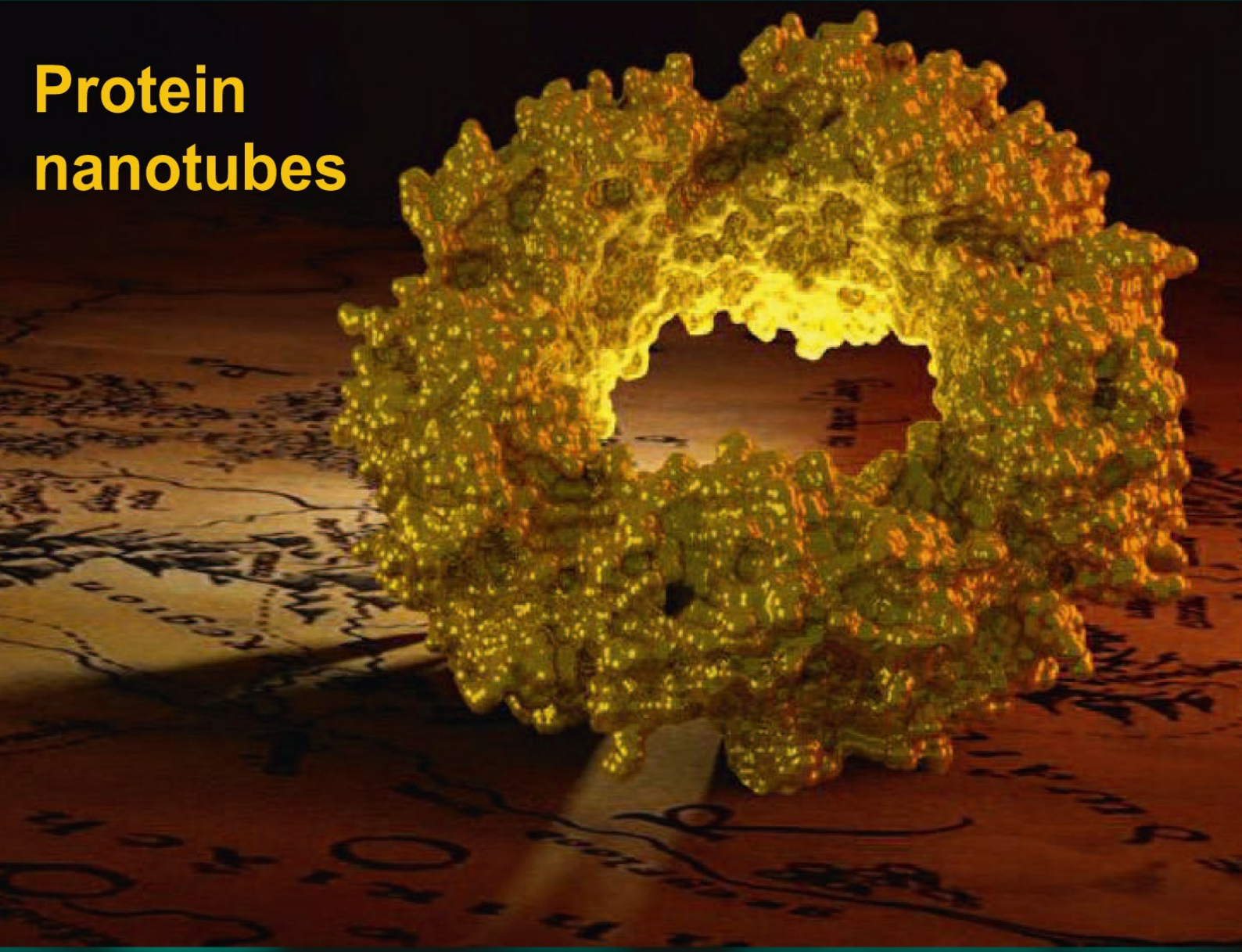

State-of-the-Art Reviews
Oncometabolites: tailoring our genes
Current understanding of LRRK2 function and dysfunction

Review Article
Nanotubes, chaperones and macromolecular crowding

the FEBS Journal
REVIEW ARTICLE

One ring (or two) to hold them all – on the structure and function of protein nanotubes

Francesco Angelucci[1,*], Andrea Bellelli[2,*], Matteo Ardini[1], Rodolfo Ippoliti[1], Fulvio Saccoccia[2] and Veronica Morea[3]

1 Department of Health, Life and Environmental Sciences, University of L'Aquila, Italy
2 Department of Biochemical Sciences 'A. Rossi Fanelli', Sapienza University of Rome and Istituto Pasteur-Fondazione Cenci Bolognetti, Rome, Italy
3 CNR – National Research Council of Italy, Institute of Molecular Biology and Pathology, Rome, Italy

Keywords
homo-oligomeric complexes; macromolecular crowding; molecular chaperones; peroxiredoxin; rosettasome; stable protein 1; symmetric macromolecular assemblies; thermosome

Correspondence
A. Bellelli or F. Angelucci, Department of Biochemical Sciences 'A. Rossi Fanelli', Sapienza University of Rome, P.le Aldo Moro 5, 00185 Roma, Italy; Department of Health, Life and Environmental Sciences, University of L'Aquila, P.le Salvatore Tommasi 1, 67100 L'Aquila, Italy
Fax: +39 06 4440062; +39 0862433414
Tel: +39 06 49910556; +39 0862433787
E-mails: andrea.bellelli@uniroma1.it; francesco.angelucci@univaq.it

*These authors contributed equally to this work

(Received 28 October 2014, revised 31 March 2015, accepted 4 June 2015)

doi:10.1111/febs.13336

Understanding the structural determinants relevant to the formation of supramolecular assemblies of homo-oligomeric proteins is a traditional and central scope of structural biology. The knowledge thus gained is crucial both to infer their physiological function and to exploit their architecture for bionanomaterials design. Protein nanotubes made by one-dimensional arrays of homo-oligomers can be generated by either a commutative mechanism, yielding an 'open' structure (e.g. actin), or a noncommutative mechanism, whereby the final structure is formed by hierarchical self-assembly of intermediate 'closed' structures. Examples of the latter process are poorly described and the rules by which they assemble have not been unequivocally defined. We have collected and investigated examples of homo-oligomeric circular arrangements that form one-dimensional filaments of stacked rings by the noncommutative mechanism *in vivo* and *in vitro*. Based on their quaternary structure, circular arrangements of protein subunits can be subdivided into two groups that we term Rings of Dimers (e.g. peroxiredoxin and stable protein 1) and Dimers of Rings (e.g. thermosome/rosettasome), depending on the sub-structures that can be identified within the assembly (and, in some cases, populated in solution under selected experimental conditions). Structural analysis allowed us to identify the determinants by which ring-like molecular chaperones form filamentous-like assemblies and to formulate a novel hypothesis by which nanotube assembly, molecular chaperone activity and macromolecular crowding may be interconnected.

Mechanisms of protein nanotubes formation

According to the classification formulated by Jean Marie Lehn [1], noncovalent assembly of supramolecular structures may occur via two different and mutually exclusive mechanisms: commutative and noncommutative. The commutative mechanism consists of the aggregation of subunits to the growing polymer, either one or more

Abbreviations
1D, one-dimensional; DoRs, Dimers of Rings; HCP1, hemolysin-corregulated protein 1; HMW, high molecular weight; Hsp, heat shock protein; LMW, low molecular weight; PDB, Protein Data Bank; Prx, peroxiredoxin; RoDs, Rings of Dimers; SP1, stable protein 1; TEM, transmission electron microscopy; TRAP, trp RNA-binding attenuation protein.

than one at a time, without a specific combination order (Fig. 1a). Conversely, the noncommutative mechanism is a hierarchical self-assembly, where intermediate polymeric structures hold the specific information required to build up the subsequent structure (Fig. 1b–d). The hierarchical nature of the latter process entails an intrinsic advantage, namely the possibility to control the overall process at several levels [2].

Homo-oligomeric (or pseudo-homo-oligomeric) proteins can have 'open' or 'closed' supramolecular

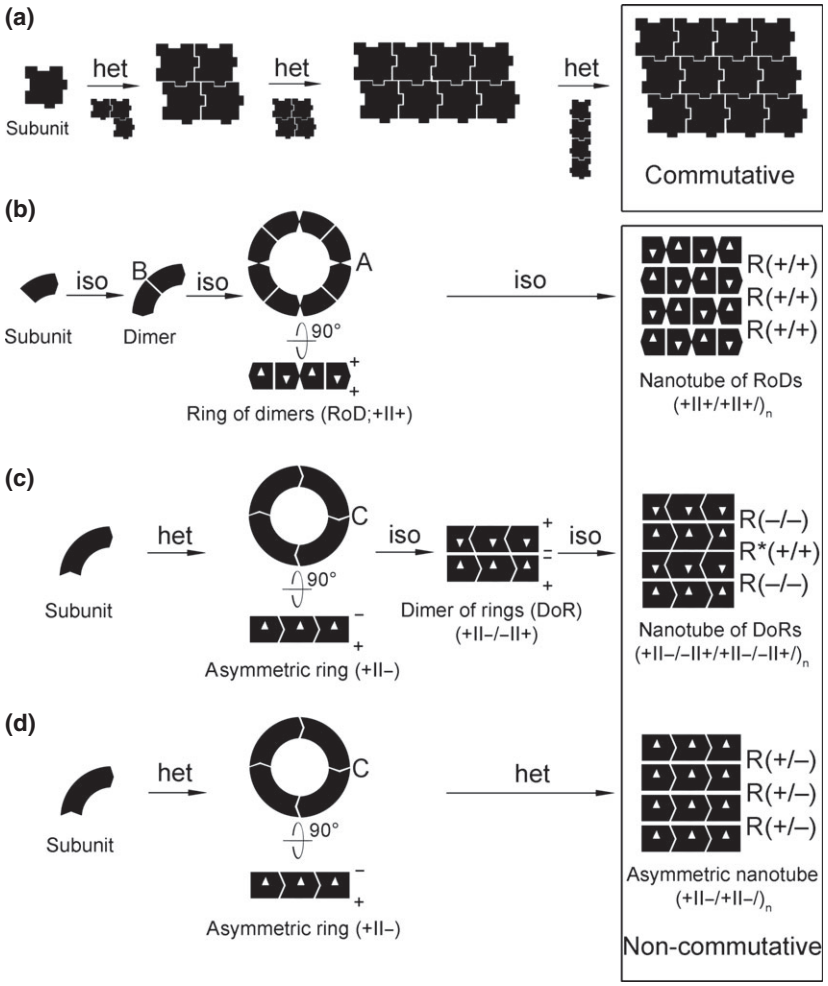

Fig. 1. Commutative and noncommutative mechanisms lead to the formation of open and closed structures. In (b) to (d) white triangles indicate the subunits asymmetric nature, resulting in different top and bottom ring surfaces; A, B and C indicate inter-subunit interfaces; R and R* indicate inter-ring interfaces. (a) Commutative mechanism: each building block can be added on a pre-formed structure without a defined order or stoichiometry (i.e. one or two or more pieces can be added at various places with each step) *via* heterologous (het) association. An open structure is generated, whose binding sites for further subunit addition are always exposed. (b) Noncommutative mechanism: generation of symmetric nanotubes via RoDs formation. Isologous (iso) binding of protein subunits leads to the formation of symmetric dimers. These bind isologously, giving rise to closed, symmetric RoDs (+II+), endowed with identical surfaces (+). The isologous inter-subunits interfaces within and between dimers are named B and A, respectively. Further isologous polymerization of RoDs generates symmetric nanotubes $(+II+/+II+)_n$, characterized by the presence of both identical surfaces (+) and isologous inter-ring R-interfaces (+/+). (c) Noncommutative mechanism: generation of asymmetric nanotubes via DoRs formation. Heterologous binding of protein subunits leads to the formation of closed, asymmetric rings (+II−), endowed with different ring surfaces (+ and −). The heterologous inter-subunit interfaces within the ring are named C. Asymmetric rings bind isologously, giving rise to symmetric DoRs (+II−/−II+) having identical surfaces (+) and isologous inter-ring R*-interfaces (–/–). DoRs can stack with one another by isologous binding giving rise to symmetric nanotubes $(+II-/-II+/+II-/-II+)_n$. These are characterized by the presence of identical surfaces (+) and of two different and alternating types of isologous R-interfaces: R*(–/–) and R(+/+). (d) Noncommutative mechanism: generation of asymmetric nanotubes via asymmetric rings formation. As in (c), heterologous binding of protein subunits leads to the formation of closed, asymmetric rings (+II−). At variance with (c), asymmetric rings assemble by heterologous binding, giving rise to asymmetric nanotubes $(+II-/+II-)_n$. These are characterized by the presence of different surfaces (+ and −) and identical, heterologous ring R-interfaces (−/+).

structures [3,4]. In open structures, the binding surface of at least one subunit is at least partially exposed, so that other subunits can subsequently bind [4]. The biological polymers generated in this way usually show helical symmetry and have a structural role (e.g. tubulin, actin, pilin, etc.) [4]; their mechanism of assembly is commutative. By contrast, in closed structures, characterized by point-group symmetries (e.g. dihedral or cyclic), all the binding surfaces of the subunits are in contact with partners; this saturates the assembly and gives rise to finite, noncommutative, structures [3]. Interface formation can be achieved via isologous or heterologous binding [5], which involve identical and different patches of residues from two interacting subunits, respectively. Consequently, heterologous binding can generate both open and closed structures, whereas isologous binding is usually associated with closed structures and can generate open structures only when each subunit comprises multiple binding sites.

We have observed that the commutative and noncommutative mechanisms are consistent with the formation of open (Fig. 1a) and closed (see ring formation step in Fig. 1b–d) structures, respectively. Closed structures (e.g. protein rings) show little tendency for further association [6], and examples of one-dimensional (1D) arrays belonging to this class have not been structurally characterized at an atomic level [2]. However, by exploiting the possibility of controlling one of the steps of the noncommutative building process, it is possible to uniformly mineralize hollow protein nanotubes by binding metals in the internal cavity of single rings before they are stacked [7]. As a result of difficulty in controlling the assembly process, the same goal would be hard to accomplish in the case of nanotubes formed by the commutative mechanism. Therefore, understanding the rules by which a noncommutative nanotube is formed appears to be of strategic importance for creating new functional architectures that may be exploited for bionanotechnological applications.

In this review, we collected and analyzed examples of homo-oligomeric circular arrangements that are known to form filaments of stacked rings by noncommutative mechanisms. We start from a theoretical analysis of symmetry requirements and constraints for ring formation, and of the structural features required for stacking with identical ring structures through either isologous or heterologous binding (Fig. 1b–d). A literature survey (Table 1) indicated that isologous interface recognition is largely prevalent and may be the only physiologically relevant mechanism of nanotube growing. The circular arrangements usually encountered were further subdivided into two groups, Rings of Dimers (RoDs) and Dimers of Rings (DoRs), depending on the specific homo-oligomeric structure of the ring and the sub-structures that can be identified within the assembly and that may or may not be populated in solution under selected experimental conditions

We noted that, amongst proteins known to form 1D arrays by a noncommutative mechanism, some functional roles are highly represented, most notably molecular chaperones. Based on structural analysis, we clarified the determinants by which specific ring-like molecular chaperones form filamentous-like assemblies and formulated an original hypothesis about the physiological roles of these supramolecular assemblies.

Nanotubes generated by noncommutative mechanisms: three possible modes of ring stacking

On the basis of symmetry considerations, some general rules are formulated to describe how protein rings, characterized by the presence of one rotational symmetry axis perpendicular to the plane of the ring, may stack forming nanotubes. In particular, we refer to protein rings made up of identical (or pseudo-identical) subunits. According to the literature, these rings may stack by three fundamental modes (Fig. 1b–d), even though there is no evidence for one of these (Fig. 1d) occurring under physiological conditions. The three modes of ring stacking arise from the possibility to have isologous versus heterologous recognition in the different oligomerization states (i.e. between subunits constituting the circular arrangements and between rings in nanotube assemblies). More complex arrangements are possible in theory (see below) but have not been observed in real structures.

The first relevant consideration is that any polypeptide chain (i.e. a protein subunit) necessarily folds into an asymmetric structure. Depending on whether subunits associate isologously or heterologously, two different types of symmetric ring structures are produced.

(a) By associating via an isologous interface (named 'B' in Fig. 1b), two subunits form a homodimer with 180° rotational symmetry. Rings can then build up by further assembling of symmetric homodimers via additional isologous interfaces (named 'A' in Fig. 1b). We call this assembly the RoDs (+||+; the '||' and '+' symbols represents a ring and one type of surface, respectively) and remark that they are characterized by very high-order symmetry. Indeed,

Table 1. Nanotubes characterized by TEM or X-ray crystallography and formed by protein asymmetric rings, DoRs or RoDs. 'II' and '/' indicate rings and inter-ring ('R')-interfaces, respectively. '+' and '−' indicate different types of surfaces. Nanotubes are formed by '*n*' repetitions of the units in parenthesis. For an explanation, see the main text and Fig. 1. ND, not determined.

Protein/function	Species [reference]	Mechanism of nanotube formation	*In vivo* concentration
Asymmetric rings: heterologous R-interfaces $(+II-/+II-/)_n$			
Trap (trp RNA-binding attenuation protein)/trancription regulator	*Bacillus Stearothermophilus* [12]	Site directed mutagenesis/disulfide bridge	ND
HCP1 (hemolysin-corregulated protein 1)/virulent factor	*Pseudomonas aeruginosa* [13]	Site directed mutagenesis/disulfide bridge	ND
DoRs: two (alternating) types of isologous R-interfaces $(+II-/-II+/+II-/-II+/)_n$			
EvpC (*Edwardsiella tarda* virulent protein)/virulent factor	*Edwardsiella tarda* [16]	Self-assembly	ND
Glutamine synthase/catalysis	*Saccharomyces cerevisiae* [19]	Self-assembly	ND
	Escherichia coli [60]	Metal-induced assembly	
Hemocyanin/oxygen binding	Octopus [61]	Self-assembly	30 $mg{\cdot}mL^{-1}$ [62]
	Keyhole limpet [61,63]		
	Haliotis tuberculata [64]		
Hemoglobin/oxygen transport	*Nereis virens* [20]	Self-assembly	80 $mg{\cdot}mL^{-1}$ [20]
Thermosome/molecular chaperone	*Pyrodictium occultum* [65]	Self-assembly	30 $mg{\cdot}mL^{-1}$ [15]
	Methanococcus thermolithotrophicus [66]		
	Sulfolobus shibatae [15]		
	Acidianus tengchongensis [10]		
GroEL/molecular chaperone	*Escherichia coli* [42]	Chemical derivatization of the surface	ND
RoDs: isologous R-interfaces $(+II+/+II+)_n$			
Peroxiredoxin/redox catalysis and molecular chaperone	Isoform III from *Bos taurus* [67]	Self-assembly	Approximately 6 $mg{\cdot}mL^{-1}$ in human erythrocyte [47]; 1% of total soluble proteins in several cultured cells [28]
	Isoform III from *Homo sapiens* [68]		
	Isoform I from *Schistosoma mansoni* [8,32]		
	Isoform II from Human erythrocyte [69]		
Putative RoDs			
SP1/molecular chaperone	*Populus tremula* [33]	Self-assembly	1% of total soluble proteins [33]

on the one hand, RoDs have one rotational symmetry axis perpendicular to the plane of the ring. This generates a ring structure with rotational symmetry = $360°/n_d$, where n_d is the number of dimers (because n_d is equivalent to $n_s/2$, where n_s is the number of subunits, the rotational symmetry of the ring can also be indicated as $720°/n_s$). On the other hand, RoDs have n_d 180° symmetry axes passing between the subunits of each homodimer plus n_d 180° symmetry axes passing between the dimers (Fig. 1b). As a consequence of the high-order symmetry for RoDs, the upper and lower surfaces of the ring are identical but rotated by $360/n_s$ with respect to each other.

(b) Any number of protein subunits may form an asymmetric ring (+||−) with $360°/n_s$ cyclic symmetry via the formation of heterologous interfaces (named 'C' in Fig. 1c–d). This type of assembly has, in principle, only the rotational symmetry axis perpendicular to the plane of the ring because the upper (+) and lower (−) surfaces of the ring differ from each other.

Second, we examine the nature of the interfaces involved in ring stacking, which we call ring ('R')-interfaces, as in Saccoccia *et al.* [8].

(a) RoDs have identical ring surfaces (+), therefore only isologous ring recognition is possible. The resulting 1D array contains identical isologous ring R-interfaces (+/+; the '/' symbol represents the ring interface), as well as identical R-surfaces (+) at the two nanotube ends (Fig. 1b).

(b) Asymmetric rings have different ring surfaces (+ and −); therefore, they can stack either isologously or heterologously (Fig. 1c,d).

Heterologous binding of rings in a head-to-tail arrangement leads to asymmetric nanotubes, having identical heterologous R(+/−)-interfaces and different R-surfaces at the ends (+ and −) (Fig. 1d). This arrangement has not yet been observed in naturally occurring protein nanotubes but can be obtained by chemical modification of protein rings (Table 1).

Isologous binding of two asymmetric rings gives rise to a structure that we call the DoRs (Figs 1c). DoRs have higher symmetry than the constituent asymmetric rings because, in addition to the rotational symmetry axis, they have n_s 180° rotational symmetry axes orthogonal to the rotational symmetry axis of the single ring(s), where n_s is the number of subunits of the DoRs (Fig. 1c and Table 2). As a consequence, in the structural arrangements for both RoDs and DoRs, the 180° rotational symmetry is generated by the presence of one isologous interface: the inter-subunits B-interface in RoDs (Fig. 1b) and the inter-ring R (−/−)-interface in DoRs (Fig. 1c).

Table 2. Major contacts taking place at oligomerization interfaces in the nanotubular assemblies of Prx and Thermosome. Secondary structure elements are indicated by 'H' (α-helices) and 'S' (β-strands) and numbered according to their occurrence in the primary structure. Amino acid residues are shown in parentheses. Apostrophes indicate secondary structure elements from different subunits. For a graphical representation of A, B, R_1, R_2, R and R* interfaces, see Fig. 2.

Oligomerization interface	Major contacts	Type of interaction
Prx[a]		
Intra-dimers: B-interface	S7/S7′	Isologous
Inter-dimers: A-interface	H3/H3′	Isologous
Inter-RoDs: R_1-interface	S2/S2″	Isologous
Inter-RoDs: R_2-interface	H2H6/H6′H2′	Isologous
Thermosome[b]		
Inter-subunits: C-interface	S2S3/S1′S25′	Heterologous
Intra-DoRs: R-interface	H5H17/H17′H5′	Isologous
Inter-DoRs: R_1*-interface	H10 (266–276)/H10′ (266–276): hydrophobic cluster (Fig. 4)	Isologous
Inter-DoRs: R_2*-interface	H10 (281–289)/H10″ (281–289): hydrophilic cluster (Fig. 4)	Isologous

[a] For a comprehensive description of the smPrx fold, see Saccoccia *et al.* [8] (contacts are shown in Fig. 5).
[b] For a comprehensive description of the Thermosome fold, see Ditzel *et al.* [18] (contacts are shown in Figs 3 and 4).

DoRs can further polymerize via isologous binding of the free (+) surfaces, forming an assembly where two types of isologous ring interfaces alternate: the R (−/−)-interface, which was already present within the DoRs, and the ring interface between DoRs, which we name R*(+/+) to distinguish it from the previous one (Fig. 1c).

Examples of both RoDs and DoRs are present in the Protein Data Bank (PDB). These include the three-dimensional structures of peroxiredoxin (Prx) RoDs [9] and thermosome, the group-II chaperonine in archaea DoRs [10]. Both of these structures are able to form nanotubes (see below).

In addition to dimers, protein subunits can generate more complex closed symmetric oligomeric structures (e.g. tetramers and octamers), which may, in principle, generate symmetric rings structures. As a result of their dihedral symmetry, rings formed by such higher-order oligomers would possess isologous ring surfaces and therefore structural properties similar to RoDs. This case has not been considered in the present review because, to the best of our knowledge, no pertinent example has been reported to date, with the possible exception of erythrocruorins and chlorocruorins [11], whose structural characterization is incomplete.

Naturally occurring noncommutative nanotubes form through isologous recognition

We analyzed the available structures of nanotubes determined by X-ray crystallography and/or electron microscopy and generated by the aggregation of protein rings by the noncommutative mechanism (Table 1). Based on their structural features, the selected nanotubes were assigned to one of the three categories described above (Fig. 1b–d).

The head-to-tail arrangement of asymmetric rings (+||−/+||−) (Fig. 1d) was detected only in the 1D assemblies of trp RNA-binding attenuation protein (TRAP) [12] and hemolysin-corregulated protein 1 (HCP1) [13] mutants. The resulting nanotubes have cyclic symmetry and are unlikely to be physiologically relevant because, in both cases, ring stacking was forced by the oxidation of cysteine residues introduced at the R(−/+)-interface by site-directed mutagenesis. It is relevant to note that stacking of TRAP rings is not specific in that both head-to-head and tail-to-tail stacking nanotubes are observed, as well as the previously mentioned head-to-tail arrangement. The ability to form assemblies whose subunits have different orientations can be ascribed to the large and poorly specific hydrophobic surface of TRAP rings and the

possibility to form disulfide bridges in all three ring orientations [12]. To our knowledge, these are peculiar features of mutated TRAP rings, and do not occur in protein rings whose nanotube assembly is physiological rather than forced on by mutagenesis.

All of the other nanotube structures available from the PDB show a head-to-head arrangement. They comprise either symmetric RoDs (+||+) (Fig. 1b) or couples of asymmetric rings (DoRs; +||−) (Fig. 1c). In both cases, the resulting nanotubes are characterized by dihedral symmetry. In addition to being most frequent, head-to-head nanotubes have a clear physiological relevance because some of them occur *in vivo*. As an example, nanotubes of Prx and Thermosome, the prototypic RoDs and DoRs structures, respectively (Fig. 2), have been observed inside cells by electron microscopy [14,15].

In Prx, both the RoDs assembly and the constituent symmetric dimers have a functional role. The RoDs structure of Prx has been described above: RoDs are generated by isologous recombination of dimers; therefore, they contain two types of isologous intra-ring interfaces (i.e. intra- and inter-dimer), named B- and A-interfaces, respectively (Fig. 2 and Table 2). Ring stacking, observed for the first time in *Schistosoma mansoni* PrxI (smPrx) occurs via identical R-interfaces [8] (see the +/+ interface in Figs 1b and 2 and Table 2) and is therefore also isologous.

From a structural point of view, the distinction between DoRs and RoDs and their higher-order 1D assemblies is unequivocal. In DoRs and DoRs-containing nanotubes, it is always possible to recognize a heterologous inter-subunit C-interface, whereas, in RoDs, only isologous inter-subunit interfaces are present (Fig. 1).

As far as the assembly process is concerned, the structures of intermediate oligomers can be hypothesized from the sub-structures identified in DoRs and RoDs, although experimental evidence is necessary to validate the hypothesis. Although the intermediate polymeric structures of typical RoDs are necessarily homodimers, in principle, DoRs may be assembled in two different ways, depending on the binding energy of the different interfaces: (a) by joining two single asymmetric rings (e.g. in Fig. 2a, the subunits of one ring are coloured red and orange, and the subunits of the other white and yellow); (b) by joining several homodimers (e.g. in Fig. 2a, the subunits of one of these homodimers are coloured orange and yellow) by an 'extended' isologous C*-interface, comprising the two heterologous but symmetrically disposed C-interfaces of the single subunits (Fig. 2a). The structure generated this way would be easily recognizable from true RoDs because the symmetry across the inter-dimer interface would involve two dimers (e.g. in Fig. 2a, orange–yellow and adjacent red–white dimers across the C*-interface), rather than two monomers as in true RoDs (e.g. in Fig. 2b, orange and red subunits across the A-interface). Experimental evidence, when available, unequivocally solves the issue.

In a few cases, there are indications that the intermediate assemblies of typical DoRs are single rings; for example, the most stable assembly of *Edwardsiella tarda* virulent protein is the single ring with non-isologous R-surfaces [16]. In the case of the DoRs GroEl, a group I chaperonine, rotation of the two stacked asymmetric rings with respect to a hypothetical 'in register' orientation (such as that shown in Fig. 2a) makes any hypothetical homodimer intermediate formation unlikely because of the reduced size of the contact surface between any two stacked monomers. In other cases, however, assemblies with molecular weight lower than the DoRs cannot be isolated. In Arthropodan hemocyanins, which only form DoRs-like assemblies but no real nanotubes, the double symmetric ring is directly in equilibrium with the isolated subunits but not with single rings [17]. Other DoRs-forming proteins, such as thermosoma, glutamine synthase and *Nereis virens* hemoglobin, are only stable as DoRs (or DoR-based nanotubes) [18–20].

In the case of RoDs-based Prx nanotubes, both the homodimer and symmetric ring can be isolated and are (or can be) populated during the catalytic cycle; consistently, the intra-dimer B-interface (Fig. 2b) is the most stable and the most difficult to dissociate [9]. Moreover the active site, endowed with thioredoxin peroxidase activity, is made up of residues from both monomers of the same dimer, and identifies the dimer as a functional unit.

Thus, where experimental evidence for intermediate assembly structures is available, true RoDs populate two characteristic species: the homodimer and the perfectly isologous and symmetric RoDs itself; conversely, DoRs populate the non-isologous single asymmetric ring. Interestingly, the available tertiary structures of proteins forming DoRs and RoDs do not show structural similarities (see below), even though evolutionary relationships have been inferred to occur between RoDs-forming Prx and the apical domain of DoRs-forming GroEL [21].

A simple way of visualizing the asymmetric ring assembly of DoRs is by imagining a group of identical children playing the popular game 'Ring a Ring o' Roses'. In this game, the children hold one another by

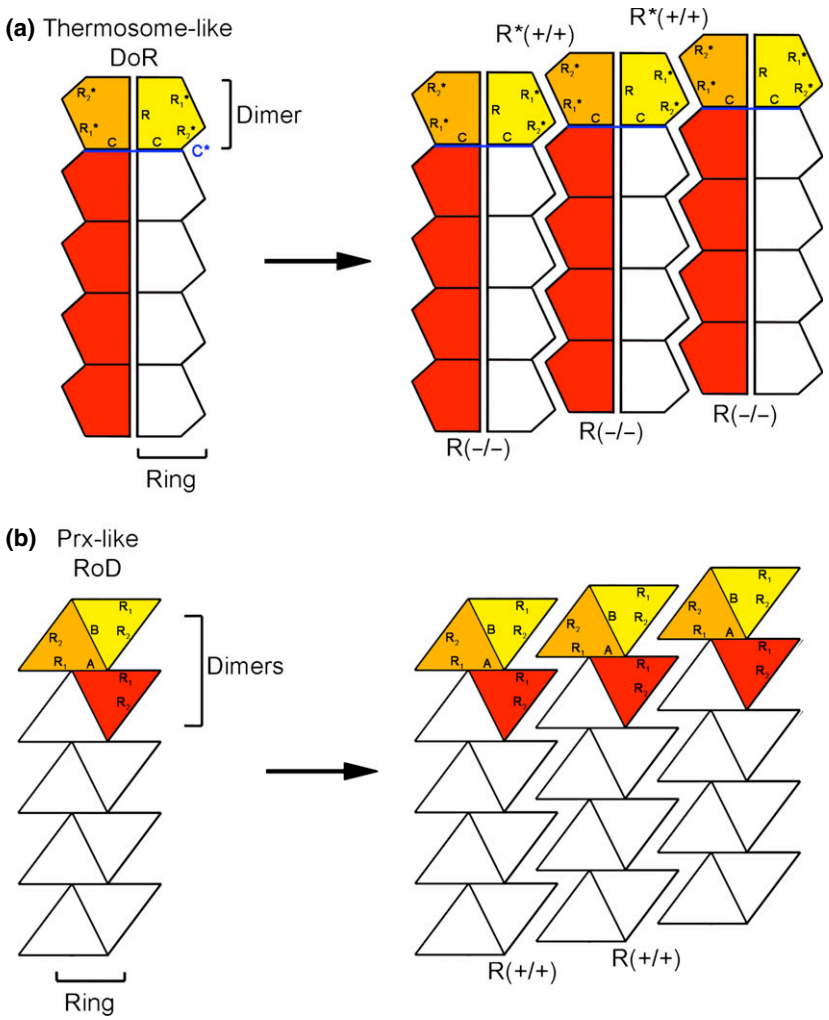

Fig. 2. Cogwheel models of DoRs and RoDs. Rings are represented by series of pawls and grooves. In known structures (Table 1), the R-interface of both DoRs and RoDs is comprised of two different, smaller interfaces, named R_1 and R_2. These are generated by isologous association of different R_1 and R_2 surfaces present in each subunit, respectively. Starting from the position shown left of the arrow (i.e. with pawls and grooves of each macromolecular assembly aligned to the equivalent features of an identical assembly), interlocking, which is a required step in nanotube formation, requires a rotation of one of the two DoRs or RoDs around the rotational symmetry axis. (a) Thermosome-like DoRs assembly. In the thermosome DoRs, the subunits of the two constituent asymmetric rings are in register and generate the R-interface. In DoRs, two possible polymeric sub-structures can be recognized: (i) single ring (orange and red) characterized by the heterologous C-interface and (ii) homodimer (orange and yellow) (see main text). The pawls of one DoRs fit into the grooves of another DoRs following a $360°/n_s$ rotation of one DoRs with respect to the other, starting from an in register position. (b) Prx-like RoDs architecture. In Prx RoDs, two different isologous interfaces are present, B and A, which identify two different homodimers: (i) orange and yellow and (ii) orange and red. In this case, a rotation of just a few degrees is sufficient for the pawls of one RoDs to interlock with the grooves of another.

hand, the right hand of each child contacting the left hand of the child nearby. The resulting ring will therefore have heterologous C-interfaces, generated by contacting right and left hands, and two different R surfaces, one made up of the children's heads (−), the other by their feet (+). This asymmetric ring has only one symmetry axis, passing through the ring centre and perpendicular to the R-surfaces, with rotation $360°/n_s$, where n_s is the number of children. Identical asymmetric rings of children playing 'Ring a Ring o' Roses' could generate either a TRAP-like arrangement or a thermosome-like DoRs. The TRAP arrangement would result from the juxtaposition of two (or more) identical groups of children one on top of the other, in whichever orientation, leading to randomly alternating head-to-feet, head-to-head and feet-to-feet interfaces

[12]. Conversely, the thermosome-like DoRs would be generated by rotating the second group of children by 180° along the symmetry axis and laying the head of each child between the heads of two children of the first ring, thus generating an isologous head-to-head R (−/−)-interface. The symmetry of the RoDs assembly can be described using this analogy as well, although a more acrobatic game should be imagined, in which the children first join in pairs. One member of each pair stands on his/her feet, the other stands on his/her head, and the two join each other by the same hand (e.g. right-to-right), generating isologous B-interfaces. Children pairs would then join to one another via left-to-left hand contacts, generating isologous A-interfaces, to form a RoDs where all children face the axis of the circle. The RoDs has $720°/n_s$ rotational symmetry (where n_s is the number of children) and two identical R-surfaces, in that they are made up of regularly alternating heads and feet. Juxtaposition of two (or more) identical RoDs would generate isologous R-interfaces.

The nanotube assemblies of DoRs and RoDs is a consequence of their dihedral symmetry, which ensures that each stereochemical feature is periodically repeated on each R-interface every $360°/n$, where n is the rotational number of the ring. This coincides with the number of monomers (n_s, as in DoRs) or dimers (n_d, as in RoDs). It is possible to assimilate DoRs and RoDs circular assemblies to cogwheels where pawls and grooves follow a periodic distribution along the R-surfaces. Both DoRs and RoDs stacking involves fitting the pawls of one ring to the grooves of the other. In both the 1D arrays, the pawl of one ring, when lodged into the groove of the other, presents two isologous surfaces that we call R_1 and R_2 (for a detailed description, see Fig. 2 and Table 2; see also below). This requires the rotation of one ring around the rotational symmetry axis to ensure surface complementarity. The extent of rotation observed in known structures of stacked thermosome-like DoRs and Prx-like RoDs is significantly different. Thermosome DoRs stacking takes place via a $360°/n_s$ rotation (where n_s is the number of subunits) between DoRs at the R*(+/+)-interface (Fig. 2a). Conversely, Prx RoDs stacking takes place via a smaller rotation (Fig. 2b) because of the slant between the B-interface and the plane of the ring.

Below, we discuss in some detail a restricted sample of the examples presented in Table 1. These were selected because the 3D structure of the nanotube assembly is available, or can be inferred from the coordinate files, and their supramolecular assemblies are likely to have functional implications.

Thermosome

A prototypic example of DoRs is represented by the thermosome also named rosettasome, a group II chaperonine (Figs 2a and 3a). The thermosome is present in the archaea domain of life, is the evolutionary precursor of TCP1 (T complex protein 1) in eukarya and acts as an ATP-dependent folding machine. DoRs functional units are built-up by isologous binding of two identical rings. Within each asymmetric ring, sub-

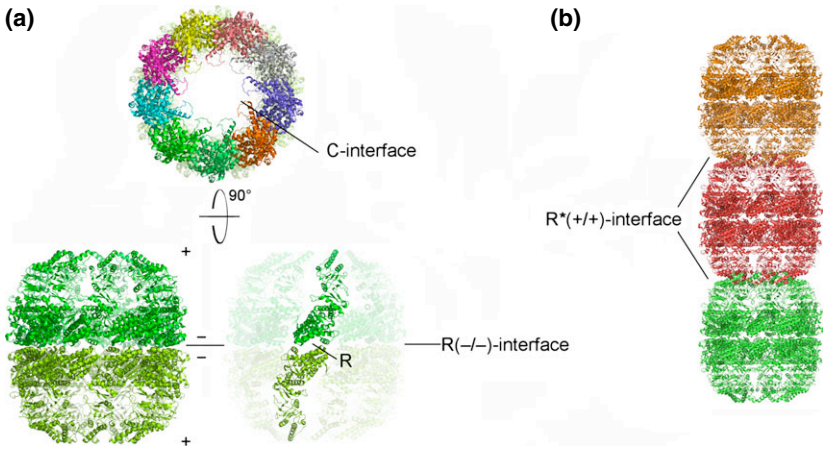

Fig. 3. Ribbon representation of *Acidianus tengchongensis* thermosome crystal structure (PDB code: 3KO1) [10]. (a) DoRs functional unit. Top: each asymmetric (+II−) ring is characterized by nine identical β-subunits (in different colours), which recognize one another by means of heterologous C-interface. Bottom: one asymmetric ring (light green) stacks with an identical ring (lime green) through the R(–/–)-interface (Table 2), giving rise to the thermosome functional assembly. (b) Nanotube present in the asymmetric unit. Three different DoRs are coloured orange, red and green, respectively. The two R*(+/+)-interfaces between DoRs are indicated.

unit recognition takes place by heterologous binding (Table 2). The structure resembles that of GroEL (group I chaperonine) except that GroEL employs a co-chaperone to fold proteins, whereas thermosome subunits contain an α-helical protrusion at the rim of the ring that works as a 'built-in' lid [22]. The thermosome comprises either or both types of pseudo-identical subunits named α and β. These have high sequence identity (approximately 50–60%) and identical patches of residues necessary to exert the physiological function [23]. Both subunits are characterized by equatorial, intermediate and apical domains, whose overall fold is the same as the respective domains of GroEL [24]. The subunit composition of the single rings varies in different species, ranging from eight to nine subunits. The entire assembly is thus characterized by D_8 or D_9 point-group symmetry. Thermosome rings can contain either identical (i.e. all α or all β) or pseudo-identical (i.e. part α and part β) subunits. C_9 rings are in general homo-oligomeric, whereas pseudo-identical subunits occur in an alternating α/β arrangement within rings characterized by C_8 (pseudo)symmetry. In the latter case, the interaction between asymmetric rings in the DoRs occurs via pairing of identical subunits (i.e. α with α and β with β). The DoRs is the thermosome functional unit; it is only possible to disassemble the thermosome double ring into lower molecular weight species under harsh and nonphysiological conditions [18].

One of the current hypotheses about the working mechanism of group II chaperonins proposes a folding mechanism similar to that of GroEL, where the substrate is released into the chamber and its folding pathway is modulated by the electrochemical environment of the protein interior. First, the substrate binds to a hydrophobic patch located on the lid, and is released into the folding chamber before lid closure. Upon ATP hydrolysis, the two asymmetric rings of the DoRs undergo an open-to-close transition. The open form is the substrate acceptor and the closed form is competent for protein folding [22]. The binding site for the unfolded peptides is proposed to be located between helices H10 and H11 on top of each ring according to Ditzel *et al.* [24] and H8 and H9 according to Huo *et al.* [10] (Fig. 4). There is a conspicuous hydrophobic patch located in the lid region, which is composed of the residues: A262, I264, I266, P269, M272, F275 and L276 (numbering according to *Acidianus tengchongensis* thermosome) [10]. In the sequence alignment of thermosome from representative species, all the above residues are highly conserved and P269 and F275 are invariant, suggesting that they are substrate binding determinants [10,22].

Several thermosomes (Table 1) are known to form 1D assemblies both *in vitro* and *in vivo*. The formation of filamentous-like structure is triggered *in vitro* by the presence of ATP or ADP, Mg^{2+} and protein concentrations above 1 $mg{\cdot}mL^{-1}$ (the *in vivo* concentration of thermosome from *Sulfolobus shibatae* may reach 30 $mg{\cdot}mL^{-1}$ (i.e. 30 μM considering the 18-mer functional assembly) [15]. Thermosomes constituted of either one (i.e. α or β) or two (i.e. α and β) types of subunits are able to stack, indicating that the structural determinants necessary for DoRs stacking are present in both the pseudo-identical subunits. However, the nature of interactions determining the nanotube architecture had not been detected.

To clarify the nature of the thermosome R*(+/+)-interface, we analyzed the recently published crystal structure of *A. tengchongensis* thermosome in the open form (PDB code: 3KO1) (Fig. 3b) [10]. The asymmetric unit contains one asymmetric 9-mers ring containing nine β-subunits and therefore is characterized by 360°/9 rotational symmetry. From this 'reference' ring, the DoRs (18-mers) can be generated by visualizing the symmetry-related ring along the nine-fold symmetry axis, which stacks with the reference ring through the isologous R(−/−)-interface. This DoRs represents the *A. tengchongensis* thermosome functional unit (i.e. the assembly endowed with molecular chaperone activity) [25] (Fig. 3a, bottom). We noted that, within the crystal lattice, another ring from a different crystallographic asymmetric unit (9-mer) was stacked with the reference ring along the nine-fold symmetry axis through an extended contacting R*(+/+)-interface (Fig. 3b). In particular, the H10 helix of one subunit of the reference ring, resembling a pawl, is wedged into the groove lined by two H10′ and H10″ helices (the apostrophes indicating different subunits), penetrating approximately 20 Å into the stacked ring (Fig. 4) and giving rise to the R*(+/+)-interface between two thermosome DoRs (Fig. 3b). Locking between DoRs is possible only in the open state of thermosome given that, in the closed form, the grooves between subunits disappear (see the closed form of thermosome from *Thermoplasma acidophilum*; PDB code: 1A6D) [24]. The fact that the open form is the competent conformation for DoRs stacking had been previously hypothesized for the *S. shibatae* thermosome [26]. The H10 helix comprises both a hydrophobic and a polar residue cluster, lying at the N- and C-terminal end, respectively (Fig. 4). The two stacked DoRs are rotated by $720°/n_s$ with respect to each other (Fig. 2). This brings one H10 helix (i.e. the pawl of the reference ring) in correspondence with the

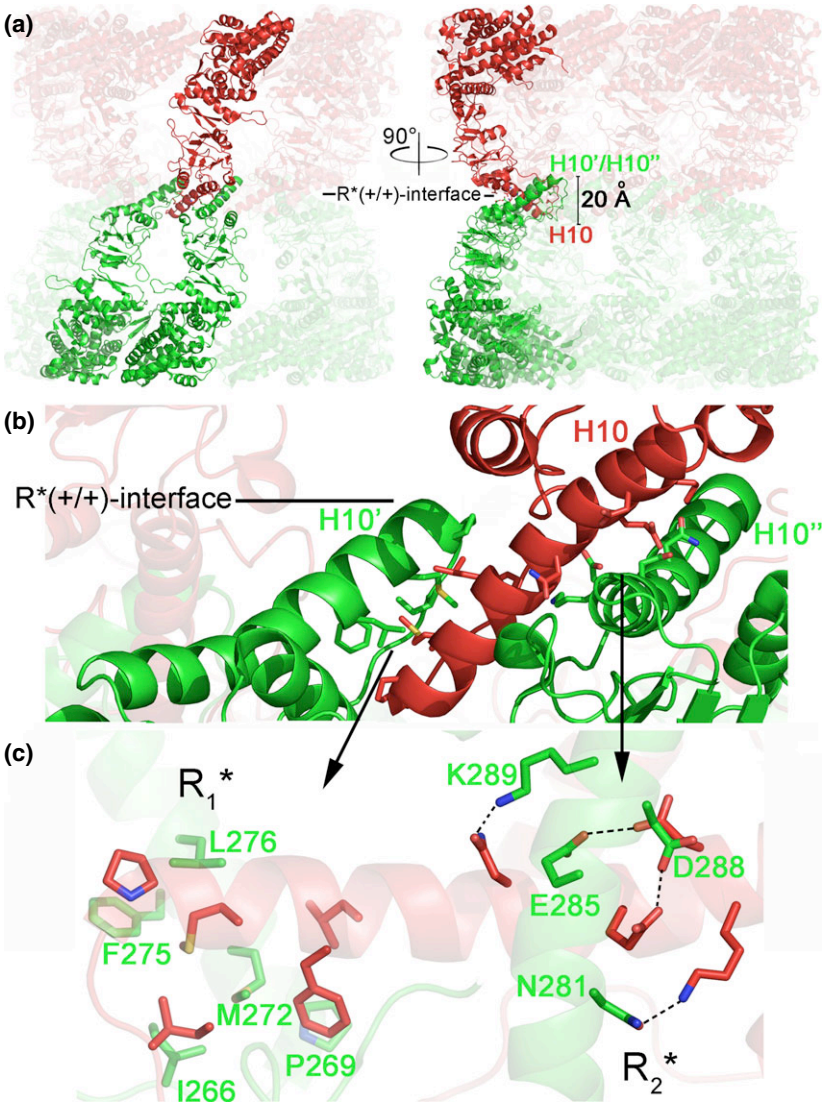

Fig. 4. Ribbon representation of thermosome regions involved in the R*(+/+)-interface between DoRs. (a) At the R*(+/+)-interface, helix H10 in the lid region of each subunit in the upper DoRs (red) acts as a pawl and penetrates approximately 20 Å into the corresponding H10 helices lining the grooves between two subunits within the bottom DoRs (green). (b) Isologous recognition between H10 helices from subunits within interlocked DoRs. (c) Stick representation of H10 helices residues taking part in isologous recognition. Colour coding is by atom type: blue, nitrogen; red, oxygen; yellow, sulfur; red and green, carbon atoms from the upper and lower DoRs, respectively. Left: the hydrophobic cluster of residues 266–276 generates the R_1-interface. Right: the hydrophilic cluster of residues 281–289 generates the R_2-interface. The dashed lines indicate the polar contacts between the residues of the two clusters, both of which are characterized by 180° symmetry.

groove of the stacked ring, which is lined by H10′ and H10″ helices (Fig. 4b). The H10′ and H10″ helices recognize the penetrating H10 helix by means of two isologous interfaces (R_1 and R_2) (Table 2), generated by their respective polar and hydrophobic clusters (Fig. 4c). The invariant residues P269 and F275 at the R*(+/+)-interface constitute the putative binding site for unfolded peptides (Fig. 4c). The calculated solvent accessible surface area that is buried at the R-interface between two thermosome DoRs is approximately 23 000 $Å^2$ (Table 3). This value is far higher than the values generally found for the 'nonbiological' crystal contacts between proteins in a crystal lattice [27], suggesting that the nanotubular architecture found in the crystal lattice of *A. tengchongensis* thermosome structure is physiologically relevant and evolutionarily selected.

Peroxiredoxin

Peroxiredoxins are ubiquitous enzymes. In eukaryotic cells, six Prx isoforms are present and classified based on cell localization and the number of cysteines involved in the enzymatic mechanism. Prx I, II, III and IV belong to the typical 2-Cys Prx subfamily. Prx I and II are cytosolic, PrxIII is mitochondrial and PrxIV is localized in the endoplasmatic reticulum. Prx I and II are considered to play alternative roles in cell physiology. Under mild oxidative stress conditions, they assemble in low molecular weight (LMW), decameric or dodecameric rings and exert thioredoxin-dependent peroxidase activity. Under high oxidative stress conditions, Prx I and II undergo a structural change to high molecular weight (HMW) forms, either nanotubes or nanoparticles, and exert a chaperone

Table 3. Quantitative analysis of R-interfaces and 'sticky' surfaces in DoRs and RoDs assemblies.

Type of assembly	DoRs		RoDs		Putative RoDs	
Protein	Thermosome		PrxI		SP1	
PDB code	3KO1		3ZVJ	Model[a]	1SI9	
Resolution (Å)	3.70		3.0	–	2.27	
R-interfaces						
Ring subunits[b]	J-R/A-I	A-I/S-0	K-T/A-J	K-T/A-J	M-Y/A-L	A-L/Q-9
Area (Å^2)[c]	8890	19 960	8060	9250	5610	5430
Percentage age polar	31	40	53	49	30	31
Percentage age nonpolar	69	60	47	51	70	69
'Sticky' surfaces[d]						
Mean area (Å^2)[e]	–	11 410	22 820	23 330	8210	8200
Percentage age polar	–	30	30	26	28	28
Percentage age nonpolar	–	70	70	74	72	72

[a] The PrxI Model was built by superimposing one of 19 identical copies of the complete G subunit onto each of the other subunits (i.e. A–F and H–T), for the majority of which one or more residues at the R-interface are not visible in the PrxI HMW structure (PDB code: 3ZVJ). Structure superposition of the main-chain atoms of residues within the common regions between all the monomers [8] was performed using INSIGHTII (BIOVIA Foundation).

[b] Ring subunits are indicated by upper-case letters corresponding to the chain identifiers in the respective PDB file.

[c] The R-interface area was calculated by subtracting the solvent accessible surface area (SASA) of two stacked rings from the sum of the SASA of the same rings in the free form. All SASA values (overall, polar and nonpolar) were calculated by NACCESS [55].

[d] 'Sticky' surfaces were defined, according to either literature data or computational predictions, to comprise specific sets of residues within subunits at R-interfaces. (a) thermosome A-I/S-0 interface: A262, I264, I266, P269, M272, P275, L276 [10,22]; (b) PrxI K-T/A-J interface [32]: P41, F46-I52, R124, K143-V145, G156, A158, F161, V162; (c) SP1 M-Y/A-L and A-L/Q-9 R-interfaces: L81–F93 (predicted by the TANGO) [37]. The thermosome J-R/A-I interface is constitutive and not endowed with chaperone activity.

[e] The 'sticky' surface area of each ring subunit was calculated as the sum of the solvent accessible surface area (SASA) of all residues belonging to the 'sticky' surface. Mean area values were calculated taking into account the 'sticky' surfaces of all ring subunits.

function by sequestering unfolded peptides and preventing their aggregation. Because of this chaperone activity is ATP-independent, Prx I and II are classified as holdases [8,28]. Notably, some typical 2-Cys Prxs are able to display holdase activity also in the decameric LMW form, under conditions where they are not subjected to stress [29]. The holdase activity of Prx was recently associated with the capability of cells to counteract stress conditions and restore protein homeostasis [30].

A mechanistic overview of the 'chameleon-like' behaviour of typical 2-Cys Prxs can be outlined. The catalytic site of these enzymes comprises the peroxidatic cysteine (Cys_p), within the N-terminal region of one subunit, and the resolving cysteine (Cys_r), at the C-terminus of a partner subunit in the homodimer. The nucleophilic attack of hydrogen (or organic) peroxide by Cys_p results in the formation of the sulfenic acid derivative Cys_p-SOH. This oxidized species can then be attacked by Cys_r, resulting in the formation of a disulfide bridge between two subunits. These subunits are part of a homodimer that, as a result of the isologous intersubunit interface, contains two identical redox sites, each composed of Cys_p within one subunit and Cys_r within the other. The shift from a reduced to oxidized state determines a weakening of the inter-dimer A-interface (Figs 2b and 5a, middle) that causes a quaternary structure transition from decamers (i.e. pentamers of dimers) to dimers. Alternatively, at high H_2O_2 concentrations, sulfenic acid derivatives might be further oxidized to sulfinic acid forms, which are not susceptible to nucleophilic attacks by Cys_r [31]. Hyperoxidation to sulfinic acid triggers secondary and tertiary structure rearrangements that cause either exposure of the binding site for unfolded peptides or, in some Prxs, a change in oligomerization state to HMW species. Recently, the first crystal structure of the HMW species of smPrxI, a typical 2-Cys Prx, has been reported, and was shown to be made up of two stacked decamers [8]. Based on this structure, a mechanism for nanotube assembly and the first 3D model whereby members of the Prx protein family form filaments of stacked rings *in vivo* [14] have been proposed [32].

The different assembly states of Prx provide a fitting example of the structures involved in the noncommutative mechanism shown in Fig. 1b. Each Prx subunit adopts the thioredoxin fold, which is made up of a β-sheet (constituted by strands S1, S2, S3, S4, S6, S7) flanked by α-helices (H1–H6). The smallest assembly that can be isolated under physiological conditions is the homodimer, which also represents the simplest quaternary structure endowed with peroxidase activity, whereas no evidence exists that isolated subunits are

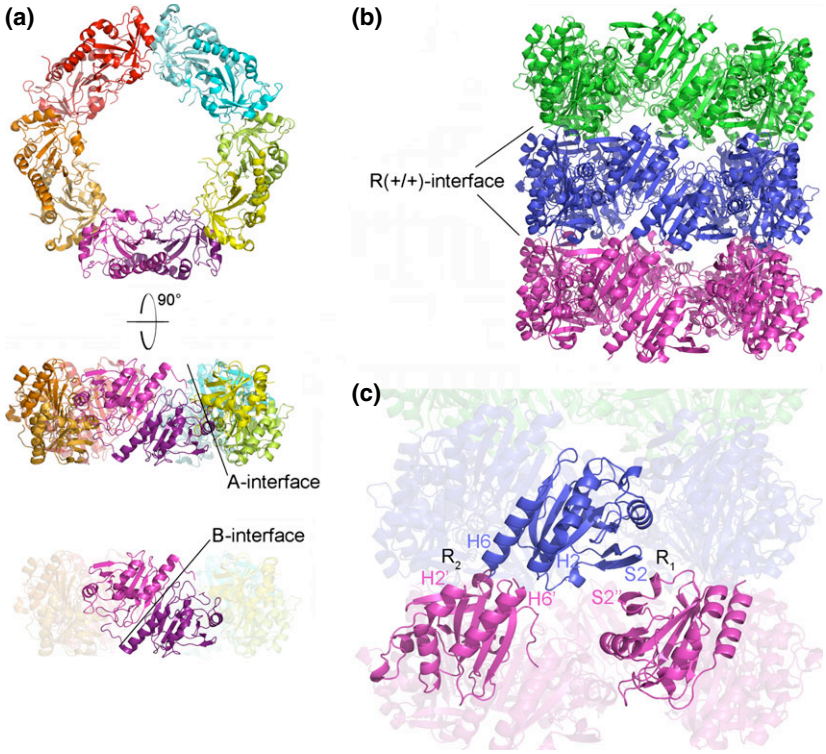

Fig. 5. Cartoon representation of *S. mansoni* Prx in different functional and aggregation states. (a) Decameric RoDs (PDB code: 3ZTL) [8]. Two subunits (e.g. coloured light and dark magenta) bind to form a homodimer through the isologous B-interface (bottom); this and four additional homodimers (light and dark yellow, cyan, red and orange, upper) bind to one another through isologous A-interfaces (middle) to close the symmetric RoDs structure (for a description of contacts at the B- and A-interfaces, see main text). (b) Model of Prx nanotube assembly. Three RoDs (coloured green, blue and magenta, respectively) stack to one another through the isologous inter-ring R(+/+)-interface. The model was built based on the first reported crystal structure of the Prx HMW form, comprising two stacked decameric RoDs (PDB code: 3ZVJ) [8]. (c) Detailed view of the R(+/+)-interface. The isologous inter-RoDs interface is made-up of two different isologous interfaces, R_1 and R_2 (Fig. 2b), generated by isologous contacts between S2 β-strands and H2/H6 α-helices, respectively.

stable under the same conditions. The homodimer is formed by two identical subunits connected via the B-interface (Figs 2b and 5a, bottom). The B-interface is isologous, built up by the joining of two S7 strands from different intra-dimer subunits in a head-to-tail manner (Table 2), and symmetric by 180° rotation, as is the homodimer (Fig. 5a, bottom). Five (or six) Prx dimers associate to form a decameric (or a dodecameric) symmetric RoDs (Fig. 1b) with D_5 (or D_6) group symmetry. The inter-dimer A-interface is constituted by H3 helices from different inter-dimer subunits, and is again isologous and symmetric by 180° rotation (Fig. 5a and Table 2). Upon chemical stimuli, two (or more) decamers stack on one another, forming the isologous R(+/+)-interface (Fig. 5b), as demonstrated for smPrxI [8]. Each subunit within a decameric RoDs fits between two subunits belonging to adjacent dimers of the stacked RoDs. As in the case of thermosome DoRs (Fig. 2a), the interaction is mediated by two isologous interfaces called R_1 and R_2 (Figs 2b and 5c). R_2 is generated by the helix dipoles of H2 and H6, and R_1 by the interaction of S2 strands (Fig. 5c and Table 2). Locking of decameric RoDs requires both a conformational change, which results in the exposure of the binding site for the unfolded peptides and a slight rotation on the five-fold symmetry axis of one decamer with respect to the other. This slight rotation (approximately 10°, F. Saccoccia, unpublished results) is visible in the crystal structure of HMW species (PDB code: 3ZVJ) [8] and is necessary to allow the isologous recognition of R_1 and R_2 as shown by the bi-dimensional (2D) models of RoDs in Fig. 2.

Stable protein 1 (SP1)

SP1 from *Populus tremula* is the best-characterized member of the plant stress-induced protein family, whose homologues have been found both in plant species and some bacteria [33]. Similar to heat shock proteins (Hsps), it is endowed with holdase activity and is

overexpressed under stress conditions. However, the SP1 sequence and structure are different from other small Hsps. It is constitutively expressed in aspens and expression levels are altered in response to several environmental stimuli. The level of SP1 expression in aspen was estimated to account for 1% of total plant proteins [33] and a similar amount was detected for Prxs I and II in eukaryotic cells [28]. SP1 is widely employed for nanotechnology purposes, especially because of its propensity to stack in nanotubes, as observed in transmission electron microscopy (TEM) micrographs [34].

SP1 subunits have a ferredoxin-like α + β sandwich fold. This consists of an antiparallel β-sheet, comprising β-strands S1–S4, which is packed with α-helices H1, H2a and H2b [35]. SP1 subunits assemble into homodimers, which were proposed to be the smallest stable units of this protein [35] (Fig. 6a).

Homodimers contain one isologous inter-subunit interface, which we name B-interface by analogy with Prxs. This is generated by association of two β-sheets, one from each subunit, into a β-barrel-like structure, the major contacts of which are contributed by strands S2S4 and S4′S2′. Homodimers assemble via inter-dimer interfaces to form dodecameric rings, whose major contacts occur between helices H1 and H1′. At variance with Prx RoDs, whose A-interfaces are entirely isologous, in SP1 rings, the interfaces between dimers also include minor heterologous contacts (Fig. 6a). However, because the interfaces between dimers are predominantly isologous, we call them A-interfaces, in analogy with Prx inter-dimer interfaces. The presence of all isologous inter-subunit interfaces is the main distinguishing feature of RoDs (Table 1). However, the assignment of the SP1 dodecameric ring

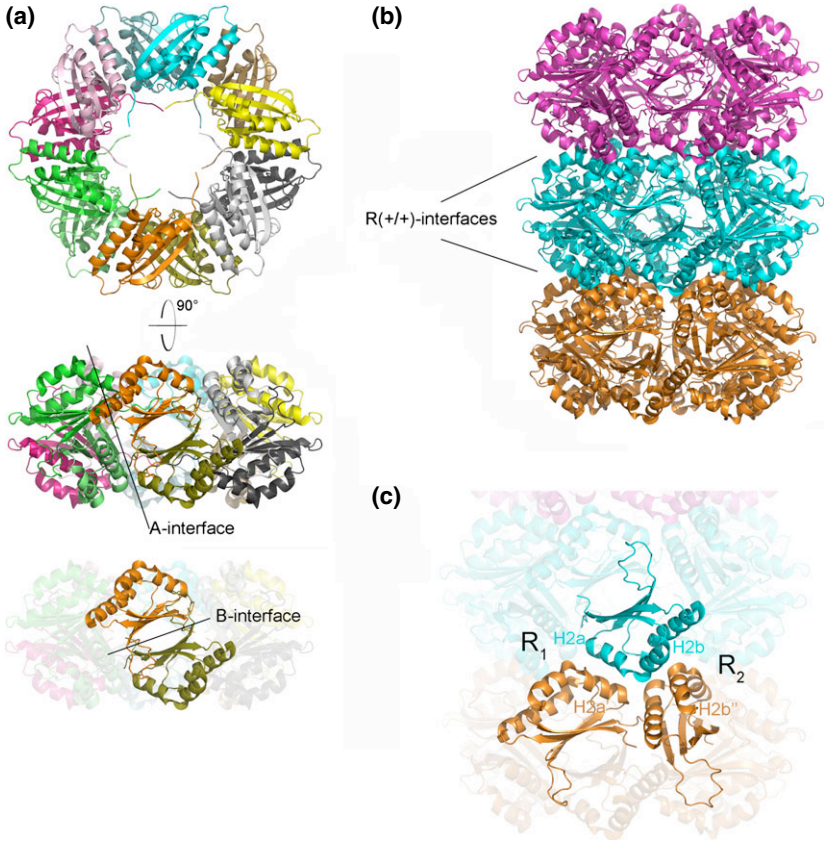

Fig. 6. Cartoon representation of *P. tremula* SP1 in different functional and aggregation states. (a) Dodecameric RoDs (PDB code: 1SI9) [34]. Two subunits (e.g. coloured light and dark orange) bind to form a homodimer through the isologous B-interface (bottom); this and five additional homodimers (light and dark green, magenta, cyan, yellow and grey, upper) bind to one another through almost entirely isologous A-interfaces (middle) to close the symmetric RoDs structure (for a description of contacts at the B- and A-interfaces, see main text). (b) Model of SP1 nanotube assembly. Three RoDs (coloured magenta, cyan and orange, respectively) stack to one another through the isologous inter-ring R(+/+)-interface. The 3D model was built following the rules for RoDs stacking revealed by the analysis of the crystal structure of *S. mansoni* Prx (Fig. 5). (c) Detailed view of the R(+/+)-interface. The isologous inter-RoDs interface is made-up of two different isologous interfaces, R_1 and R_2 (Fig. 2b), generated by isologous contacts between α-helices H2a and H2b, respectively.

to RoDs should be considered provisional because of the presence of minor heterologous contacts within inter-dimer interfaces and the stability of the dodecameric ring (Fig. 6a), which does not dissociate into either homodimeric species (as would be expected of RoDs) or single rings (as would be expected of DoRs), and only disassembles into isolated subunits after boiling in the presence of SDS [34].

Despite the available structural and functional information about SP1, the binding sites for the unfolded peptides have not been identified. Additionally, SP1 high-order oligomers have been observed in 2D TEM micrographs [34,36], although their three-dimensional structures at the atomic level are unknown. We built an atomic model of *P. tremula* SP1 1D assembly (Fig. 6b) by applying the features of RoDs interlocking that we had discovered by analyzing the nanotube model of the Prx HMW form (Fig. 5b). Accordingly, we treated RoDs subunits as pawls and grooves and juxtaposed two RoDs in such a way that the pawls of one RoDs were located into the grooves generated by two different subunits of the RoDs stacked to it. To achieve this interlocking, just a few degrees rotation of one ring with respect to the other were required, similar to that observed in the crystal structure of the two smPrxI stacked rings. The resulting 3D model of stacked RoDs is shown in Fig. 6b. As in the case of smPrxI, two isologous interfaces can be recognized within the inter-RoDs R(+/+)-interface [i.e. R_1 (whose major contact region is H2a/H2a′) and R_2 (whose major contact region is H2b/H2b″)], which are generated by a hydrophilic and a hydrophobic cluster, respectively (Fig. 6c). We used TANGO [37] to predict that the SP1 segment with the highest aggregation tendency, a property correlated with the capacity of binding unfolded peptides [38]. The predicted segment (Table 3) overlaps with the H2b region, one of the patches that appear to be involved in ring stacking. This comprises some of the exposed hydrophobic residues most conserved in the SP1 family (i.e. A84, A85, A87 and A88) [33] and is located at the rim of the ring, in analogy with other well-studied molecular chaperones characterized by a circular arrangement [32,39–41].

Possible selective advantages of noncommutative symmetric nanotubes

Do the structural features observed in this survey correlate with particular functions of the protein rings? A comprehensive physiological reason why proteins reported in Table 1 form nanotubes has not been found in the literature. Additionally, in some cases, ring stacking may be an artifact as a result of sample dehydration for X-ray and electron microscopy studies. However, thermosome and Prx rings are known to stack *in vivo* and, together with SP1, they are able to bind non-native peptides exerting molecular chaperone activity (GroEL will not be considered in the subsequent discussion because its nanotubular structure has been forced by derivatization of the R-interface [42] and therefore it is unlikely to have functional roles *in vivo*). The predominant function of proteins capable of spontaneous self-assembly into noncommutative nanotubes of either DoRs or RoDs is chaperone activity. Other physiological functions consistently present in these proteins are O_2 transport and redox catalysis. A relationship between molecular chaperone activity and aggregation tendency has already been found for the nonphysiological isolated apical domain of GroEL [38].

Why do ring-forming molecular chaperones assemble into filaments along the rotational symmetry axis? These proteins have similar function, in that they recognize unfolded peptides either to keep them in solution (RoDs forming SP1 and Prx are ATP-independent chaperones, working exclusively as holdases) or re-fold them (DoRs forming thermosome is an ATP-dependent molecular chaperone working as foldase), although their subunits are unrelated from a structural point of view. According to the Structure Classification of Proteins (SCOP) database [43], SP1, Prx and thermosome have different folds, namely ferredoxin, thioredoxin and GroEL equatorial domain-like fold, respectively. Nevertheless, their circular assemblies share several common features: (a) both DoRs-based ATP-dependent chaperones and RoDs-based ATP-independent chaperones have R-surfaces that drive ring stacking through hydrophobic and hydrophilic interactions; (b) both DoRs and RoDs exert the molecular chaperone function thanks to the exposure of 'sticky' surfaces able to bind non-native peptides [10,22,32] (Table 3); and (c) upon both DoRs and RoDs stacking, the 'sticky' surfaces become inaccessible to unfolded peptides.

As shown in Table 3, the identified 'sticky' surfaces contain extended hydrophobic regions, in agreement with previous reports about the involvement of hydrophobic surfaces in chaperone activity [44]. Intriguingly, we found that the ratio between nonpolar and polar regions is essentially invariant (approximately 70%) among 'sticky' surfaces of different proteins, despite the larger differences observed for whole R-interfaces (ranging from 50% to 70%). Although 'sticky' surfaces have been defined for just a small number of

proteins, such a high value of hydrophobic/hydrophilic surfaces may be a common feature of regions endowed with chaperone activity.

The periodic presence of hydrophobic patches was previously proposed to be a general feature shared by circularly arranged molecular chaperones allowing them to exert their function [39–41]. Indeed, this feature assures both high affinity and multivalent binding of non-native peptides. As stated above, the circular arrangement and periodicity of complementary surfaces is also a requisite to allow stacking of DoRs and RoDs. Given that the same cause (hydrophobic patches periodically distributed on the rim of the ring) can imply two effects, one functional (chaperone activity) and the other structural (ring stacking), it may be argued that the latter is a side effect of the former. Thus, under physiological conditions, ring stacking would sequester the peptide binding surfaces and would be a limiting factor of the holdase/foldase activity of these proteins. However, the prominence of noncommutative nanotube structures observed in many cell types [14,15] suggests that, at least under some conditions, the higher-order oligomers are functionally significant.

In their natural *milieu*, several molecules of different chemical nature surround proteins and this crowded environment can considerably induce aggregation. Recently, it was demonstrated that there is an inverse correlation between protein expression and exposure of 'sticky' surfaces [45] as a result of the need to prevent unspecific interactions. According to this observation, *in vivo* gene expression inversely correlates with *in vitro* aggregation propensity of the resulting proteins [46]. Molecular chaperones and shock proteins challenge this rule because they must be both present in large amount and expose 'sticky' surfaces to exert their function. Prx, thermosome and SP1 are amongst the most abundant proteins in the cytosol. As an example, PrxII decamers and thermosome 18-mers may reach a concentration of 27 μM in erythrocytes (6 $mg{\cdot}mL^{-1}$) [47] and 30 μM in archaea (30 $mg{\cdot}mL^{-1}$) [15], respectively, and SP1 represents 1% of the total soluble protein in *P. tremula* [33]. Holdase and foldase chaperones are characterized by substrate promiscuity, being able to recognize several protein substrates by their 'sticky' patches. We suggest that, under conditions where this action is not required, their promiscuity could be harmful and better kept in a quiescent status. The ring propensity to stack and consequent hiding of substrate binding sites effectively avoids unwanted substrate recognition. On the other hand, protein nanotubes can be disassembled into functional RoDs or DoRs under stress conditions and/or as a result of high concentrations of unfolded peptides. A relevant observation is that 1D assemblies, such as soluble nanotubes, are less stable than 2D and 3D lattices and can be easily dissociated into their constituent rings [48,49]. Thus, as previously suggested for the thermosome [15], nanotube formation would represent an ingenious and fully reversible mechanism to satisfy two opposite requirements of the cell, namely having high concentrations of soluble and ready to act chaperones at the same time as keeping them in a harmless state (Fig. 7). This inverse correlation between ring stacking and chaperone function has been observed *in vitro* for smPrxI. An active site mutant of this protein that is able to constitutively form long nanotubular structures (up to

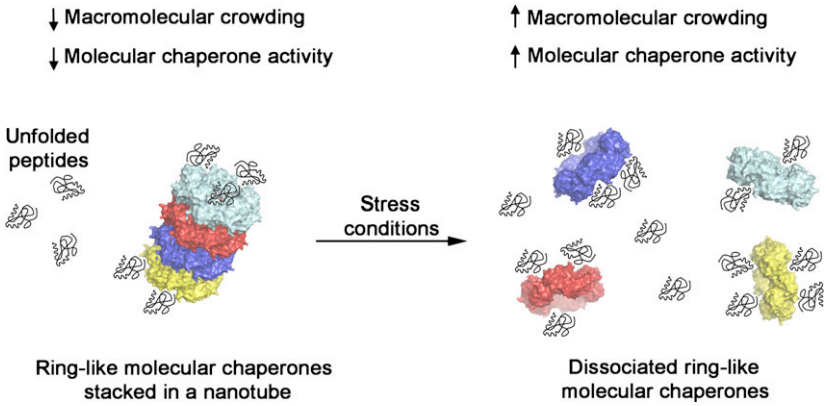

Fig. 7. Ring-like molecular chaperones in nanotube assemblies and in the free state. Left: only the exposed surfaces of rings at the extremities of nanotubes are able to interact with unfolded peptides, with the majority of binding sites for unfolded peptides being involved in ring-stacking. Right: when unfolded peptides concentrations increase (e.g. stress conditions), nanotubes dissociate into their constituent RoDs (or DoRs). The increased concentration of active molecular chaperones boosts both macromolecular crowding inside the cell and the capability to keep the unfolded proteins in solution.

approximately 100 nm; i.e. 20 stacked rings) showed a lower holdase activity than other protein variants endowed with a lower propensity to stack [32]. The hypothesis hereby presented for chaperonines and holdases is reminiscent of the mechanism of action of some small heat shock proteins. In the high-order oligomeric state, small Hsps have no holdase activity because the hydrophobic patches necessary to keep client proteins in solution are hidden after subunit aggregation. Under stress conditions and/or in presence of client proteins, small Hsps disassemble into sub-oligomeric species, which bind to unfolded peptides preventing their aggregation [50].

In addition to being supramolecular aggregation states that cells can use to switch off the molecular chaperone activity, when unnecessary, the ability of nanotubes to undergo polymerization/depolymerization equilibria may affect macromolecular crowding and, consequently, the solvent volume available to other macromolecules (i.e. excluded volume) [51]. It has been estimated by theoretical calculations that a 10% increase in the total intracellular concentration of macromolecules would cause an up to 10-fold increase in their activity [52], and the association–dissociation equilibrium of protein superstructures has been calculated to have a relevant effect on macromolecular crowding [53]. Indeed, the dissociation of tubulin, which is present at a concentration of 5.5 $mg{\cdot}mL^{-1}$ inside the cytoplasm, has been shown to have a major role in osmotic pressure modulation [54]. Proteins able to form DoRs or RoDs, and associate into nanotubes, are among the most highly concentrated in living cells (Table 1). For example, the estimated concentrations of PrxII (in erythrocytes) and thermosome (in archaeal cytoplasm) are 6 and > 30 $mg{\cdot}mL^{-1}$, respectively (see above). Thus, their polymerization/depolymerization equilibria may be estimated to cause effects not much smaller than those attributed to tubulin.

The large effects of protein association–dissociation equilibria on the activity of intracellular solutes is a result of two factors: the change of the concentration of osmotically active macromolecules and the binding or release of water molecules from their interfaces. A minimal estimate of the water mobilized upon Prx or thermosome nanotube assembly/disassembly may be calculated approximately for the first layer of solvent required to hydrate the ring interface surfaces. Prx R-interface (Fig. 1b) and thermosome R*-interface (Fig. 1c) areas coincide with the solvent accessible surface area of RoDs and DoRs, respectively, which is buried upon stacking (Table 3). This area was calculated with NACCESS [55] for the crystal structures of smPrxI (PDB code: 3ZVJ) [8] and *A. tengchongensis* thermosome (PDB code: 3KO1) [10]. To estimate the number of water molecules bound to free RoDs and DoRs ring-surfaces and excluded upon interface formation, the area of the R- and R*-interfaces was divided by the largest area occupied by a water molecule, approximated by the area of the largest section of a sphere with radius 1.4 Å. The number of water molecules bound to one RoDs or DoRs was then multiplied by the estimated *in vivo* concentration of these assemblies (i.e. 30 μM for the thermosome 18-mer DoRs and 27 μM for the Prx 10-mer RoDs; see above) to obtain the concentration of water molecules that would be released upon a hypothetical transition involving all thermosome DoRs or Prx RoDs from a state where they are all present as single or double rings to a state where they are all within their nanotube assembly. According to this estimate, thermosome or Prx nanotubes formation/disassembly would lower/raise the water activity within the cell by 0.05–0.1 M, corresponding to the release of 0.12 $g_{(H2O)}{\cdot}g_{(Prx)}{}^{-1}$ and 0.05 $g_{(H2O)}{\cdot}g_{(thermosome)}{}^{-1}$ upon nanotube formation. This amount of water may appear small; however, to give a term of comparison, we may consider that the erythrocyte contains approximately 6 $mg{\cdot}mL^{-1}$ Prx and 300 $mg{\cdot}mL^{-1}$ hemoglobin, whose allosteric structural change requires between 20 and 60 molecules of water per hemoglobin tetramer [56,57], corresponding to 0.006–0.016 $g_{(H2O)}{\cdot}g_{(hemoglobin)}{}^{-1}$. Thus, the water required to hydrate all the R-interfaces of Prx rings would be between one half and one-sixth of that required by the allosteric structural change of all the hemoglobin in the erythrocyte.

The increase in macromolecular crowding and consequent decrease of available solvent volume is reputed to have positive effects on the stabilization of protein native states [58,59]. Therefore, the two effects of disassembly of both RoDs and DoRs nanotube filaments, namely the increase of molecular chaperone activity triggered by the exposure of binding sites for unfolded peptides and the increment of molecular crowding, would represent two synergistic strategies adopted by cells to circumvent stress conditions to maintain protein homeostasis (Fig. 7).The increase in macromolecular crowding and consequent decrease of available solvent volume is reputed to have positive effects on the stabilization of protein native states [58,59]. Therefore, the two effects of disassembly of both RoDs and DoRs nanotube filaments, namely the increase of molecular chaperone activity triggered by the exposure of binding sites for unfolded peptides and the increment of molecular crowding, would represent two synergistic strategies adopted by cells to circumvent stress conditions to maintain protein homeostasis (Fig. 7).

Acknowledgements

The present review is dedicated to our friend and colleague Dr Giampiero Tempera, who died prematurely in December 2014. We are grateful to Professor Stefano Gianni (Sapienza University of Rome, Italy) for helpful discussions. The research leading to these results has received funding from the European Community's Seventh Framework Programme (FP7/2007-2013) under BioStruct-X (grant agreement No. 283570) and from Sapienza University of Rome 'Ricerche Universitarie' 2013 and 2014 to A.B.

Author contributions

F. Angelucci and A. Bellelli formulated the original ideas and general plan of the review; with the help of V. Morea they wrote down the general rules of the ring assembly. M. Ardini, R. Ippoliti and F. Saccoccia found, selected and investigated the appropriate examples of DoRs and RoDs. V. Morea carried out all the bioinformatic analysis.

References

1 Lehn JM (2002) Toward complex matter: supramolecular chemistry and self-organization. *Proc Natl Acad Sci USA* **99**, 4763–4768.
2 Rajagopal K & Schneider JP (2004) Self-assembling peptides and proteins for nanotechnological applications. *Curr Opin Struct Biol* **14**, 480–486.
3 Goodsell DS & Olson AJ (2000) Structural symmetry and protein function. *Annu Rev Biophys Biomol Struct* **29**, 105–153.
4 Lesk AM (2010) Introduction to Protein Science: Architecture, Function, and Genomics. Oxford University Press, New York.
5 Monod J, Wyman J & Changeux JP (1965) On the nature of allosteric transitions: a plausible model. *J Mol Biol* **12**, 88–118.
6 Ponstingl H, Kabir T, Gorse D & Thornton JM (2005) Morphological aspects of oligomeric protein structures. *Prog Biophys Mol Biol* **89**, 9–35.
7 Ardini M, Giansanti F, Di Leandro L, Pitari G, Cimini A, Ottaviano L, Donarelli M, Santucci S, Angelucci F & Ippoliti R (2014) Metal-induced self-assembly of Peroxiredoxin as a tool for sorting ultrasmall gold nanoparticles into one-dimensional clusters. *Nanoscale* **6**, 8052–8061.
8 Saccoccia F, Di Micco P, Boumis G, Brunori M, Koutris I, Miele AE, Morea V, Sriratana P, Williams DL, Bellelli A *et al.* (2012) Moonlighting by different stressors: crystal structure of the chaperone species of a 2-Cys peroxiredoxin. *Structure* **20**, 429–439.
9 Wood ZA, Schröder E, Robin Harris J & Poole LB (2003) Structure, mechanism and regulation of peroxiredoxins. *Trends Biochem Sci* **28**, 32–40.
10 Huo Y, Hu Z, Zhang K, Wang L, Zhai Y, Zhou Q, Lander G, Zhu J, He Y, Pang X *et al.* (2010) Crystal structure of group II chaperonin in the open state. *Structure* **18**, 1270–1279.
11 Royer WE Jr, Sharma H, Strand K, Knapp JE & Bhyravbhatla B (2006) Lumbricus erythrocruorin at 3.5 A resolution: architecture of a megadalton respiratory complex. *Structure* **14**, 1167–1177.
12 Miranda FF, Iwasaki K, Akashi S, Sumitomo K, Kobayashi M, Yamashita I, Tame JR & Heddle JG (2009) A self-assembled protein nanotube with high aspect ratio. *Small* **18**, 2077–2084.
13 Ballister ER, Lai AH, Zuckermann RN, Cheng Y & Mougous JD (2008) *In vitro* self-assembly of tailorable nanotubes from a simple protein building block. *Proc Natl Acad Sci USA* **105**, 3733–3738.
14 Phalen TJ, Weirather K, Deming PB, Anathy V, Howe AK, van der Vliet A, Jönsson TJ, Poole LB & Heintz NH (2006) Oxidation state governs structural transitions in peroxiredoxin II that correlate with cell cycle arrest and recovery. *J Cell Biol* **175**, 779–789.
15 Trent JD, Kagawa HK, Yaoi T, Olle E & Zaluzec NJ (1997) Chaperonin filaments: the archaeal cytoskeleton? *Proc Natl Acad Sci USA* **94**, 5383–5388.
16 Jobichen C, Chakraborty S, Li M, Zheng J, Joseph L, Mok YK, Leung KY & Sivaraman J (2010) Structural basis for the secretion of EvpC: a key type VI secretion system protein from *Edwardsiella tarda*. *PLoS One* **5**, e12910.
17 Hartmann H & Decker H (2002) All hierarchical levels are involved in conformational transitions of the 4 x 6-meric tarantula hemocyanin upon oxygenation. *Biochim Biophys Acta* **1601**, 132–137.
18 Waldmann T, Nitsch M, Klumpp M & Baumeister W (1995) Expression of an archaeal chaperonin in *E. coli*: formation of homo- (alpha, beta) and hetero-oligomeric (alpha+beta) thermosome complexes. *FEBS Lett* **376**, 67–73.
19 He YX, Gui L, Liu YZ, Du Y, Zhou Y, Li P & Zhou CZ (2009) Crystal structure of *Saccharomyces cerevisiae* glutamine synthetase Gln1 suggests a nanotube-like supramolecular assembly. *Proteins* **76**, 249–254.
20 Harris JR, Hoeger U & Adrian M (2001) Transmission electron microscopical studies on some haemolymph proteins from the marine polychaete *Nereis virens*. *Micron* **32**, 599–613.
21 Dekker C, Willison KR & Taylor WR (2011) On the evolutionary origin of the chaperonins. *Proteins* **79**, 1172–1192.
22 Yébenes H, Mesa P, Muñoz IG, Montoya G & Valpuesta JM (2011) Chaperonins: two rings for folding. *Trends Biochem Sci* **36**, 424–432.

23 Nitsch M, Klumpp M, Lupas A & Baumeister W (1997) The thermosome: alternating alpha and beta-subunits within the chaperonin of the archaeon *Thermoplasma acidophilum*. *J Mol Biol* **267**, 142–149.
24 Ditzel L, Löwe J, Stock D, Stetter KO, Huber H, Huber R & Steinbacher S (1998) Crystal structure of the thermosome, the archaeal chaperonin and homolog of CCT. *Cell* **93**, 125–138.
25 Wang L, Hu ZJ, Luo YM, Huo YW, Ma Q, He YZ, Zhang YY, Sun F & Dong ZY (2010) Distinct symmetry and limited peptide refolding activity of the thermosomes from the acidothermophilic archaea Acidianus tengchongensis S5(T). *Biochem Biophys Res Commun* **393**, 228–234.
26 Li Y, Paavola CD, Kagawa H, Chan SL & Trent JD (2007) Mutant chaperonin proteins: new tools for nanotechnology. *Nanotechnology* **18**, 455101–455110.
27 Levy ED & Teichmann S (2013) Structural, evolutionary, and assembly principles of protein oligomerization. *Prog Mol Biol Transl Sci* **117**, 25–51.
28 Rhee SG & Woo HA (2011) Multiple functions of peroxiredoxins: peroxidases, sensors and regulators of the intracellular messenger H2O2, and protein chaperones. *Antioxid Redox Signal* **15**, 781–794.
29 Park JW, Piszczek G, Rhee SG & Chock PB (2011) Glutathionylation of peroxiredoxin I induces decamer to dimers dissociation with concomitant loss of chaperone activity. *Biochemistry* **50**, 3204–3210.
30 MacDiarmid CW, Taggart J, Kerdsomboon K, Kubisiak M, Panascharoen S, Schelble K & Eide DJ (2013) Peroxiredoxin chaperone activity is critical for protein homeostasis in zinc-deficient yeast. *J Biol Chem* **288**, 31313–31327.
31 Hall A, Karplus PA & Poole LB (2009) Typical 2-Cys peroxiredoxins–structures, mechanisms and functions. *FEBS J* **276**, 2469–2477.
32 Angelucci F, Saccoccia F, Ardini M, Boumis G, Brunori M, Di Leandro L, Ippoliti R, Miele AE, Natoli G, Scotti S *et al.* (2013) Switching between the alternative structures and functions of a 2-Cys peroxiredoxin, by site-directed mutagenesis. *J Mol Biol* **425**, 4556–4568.
33 Wang WX, Pelah D, Alergand T, Shoseyov O & Altman A (2002) Characterization of SP1, a stress-responsive, boiling-soluble, homo-oligomeric protein from aspen. *Plant Physiol* **130**, 865–875.
34 Wang WX, Dgany O, Wolf SG, Levy I, Algom R, Pouny Y, Wolf A, Marton I, Altman A & Shoseyov O (2006) Aspen SP1, an exceptional thermal, protease and detergent-resistant self-assembled nano-particle. *Biotechnol Bioeng* **95**, 161–168.
35 Dgany O, Gonzalez A, Sofer O, Wang W, Zolotnitsky G, Wolf A, Shoham Y, Altman A, Wolf SG, Shoseyov O *et al.* (2004) The structural basis of the thermostability of SP1, a novel plant (*Populus tremula*) boiling stable protein. *J Biol Chem* **279**, 51516–51523.
36 Medalsy I, Dgany O, Sowwan M, Cohen H, Yukashevska A, Wolf SG, Wolf A, Koster A, Almog O, Marton I *et al.* (2008) SP1 protein-based nanostructures and arrays. *Nano Lett* **8**, 473–477.
37 Fernandez-Escamilla AM, Rousseau F, Schymkowitz J & Serrano L (2004) Prediction of sequence-dependent and mutational effects on the aggregation of peptides and proteins. *Nat Biotechnol* **22**, 1302–1306.
38 Chen J, Yagi H, Sormanni P, Vendruscolo M, Makabe K, Nakamura T, Goto Y & Kuwajima K (2012) Fibrillogenic propensity of the GroEL apical domain: a Janus-faced minichaperone. *FEBS Lett* **586**, 1120–1127.
39 Chatellier J, Hill F & Fersht AR (2000) From minichaperone to GroEL 2: importance of avidity of the multisite ring structure. *J Mol Biol* **304**, 883–896.
40 Farr GW, Furtak K, Rowland MB, Ranson NA, Saibil HR, Kirchhausen T & Horwich AL (2000) Multivalent binding of nonnative substrate proteins by the chaperonin GroEL. *Cell* **100**, 561–573.
41 Siegert R, Leroux MR, Scheufler C, Hartl FU & Moarefi I (2000) Structure of the molecular chaperone prefoldin: unique interaction of multiple coiled coil tentacles with unfolded proteins. *Cell* **103**, 621–632.
42 Biswas S, Kinbara K, Niwa T, Taguchi H, Ishii N, Watanabe S, Miyata K, Kataoka K & Aida T (2013) Biomolecular robotics for chemomechanically driven guest delivery fuelled by intracellular ATP. *Nat Chem* **5**, 613–620.
43 Murzin AG, Brenner SE, Hubbard T & Chothia C (1995) SCOP: a structural classification of proteins database for the investigation of sequences and structures. *J Mol Biol* **247**, 536–540.
44 Horwich AL, Fenton WA, Chapman E & Farr GW (2007) Two families of chaperonin: physiology and mechanism. *Annu Rev Cell Dev Biol* **23**, 115–145.
45 Yang JR, Liao BY, Zhuang SM & Zhang J (2012) Protein misinteraction avoidance causes highly expressed proteins to evolve slowly. *Proc Natl Acad Sci USA* **109**, E831–E840.
46 Tartaglia GG, Pechmann S, Dobson CM & Vendruscolo M (2007) Life on the edge: a link between gene expression levels and aggregation rates of human proteins. *Trends Biochem Sci* **32**, 204–206.
47 Moore RB, Mankad MV, Shriver SK, Mankad VN & Plishker GA (1991) Reconstitution of Ca(2+)-dependent K+ transport in erythrocyte membrane vesicles requires a cytoplasmic protein. *J Biol Chem* **266**, 18964–18968.
48 Brodin JD, Carr JR, Sontz PA & Tezcan FA (2014) Exceptionally stable, redox-active supramolecular protein assemblies with emergent properties. *Proc Natl Acad Sci USA* **111**, 2897–2902.
49 Chirut D, Jureschi CM, Linares J, Garcia Y & Rotaru A (2014) Lattice architecture effect on the cooperativity

of spin transition coordination polymers. *J Appl Phys* **115**, 053523.
50 Nakamoto H & Vígh L (2007) The small heat shock proteins and their clients. *Cell Mol Life Sci* **64**, 294–306.
51 Zimmerman SB & Trach SO (1991) Estimation of macromolecule concentrations and excluded volume effects for the cytoplasm of *Escherichia coli*. *J Mol Biol* **222**, 599–620.
52 Minton AP (2000) Implication of macromolecular crowding for protein assembly. *Curr Opin Struct Biol* **10**, 34–39.
53 Hall D (2006) Protein self-association in the cell: a mechanism for fine tuning the level of macromolecular crowding? *Eur Biophys J* **35**, 276–280.
54 Charmasson R (1981) Osmotic effects of tubulin (brain contractile protein) polymerization. A possible role in cell salt and water regulation. *Physiol Chem Phys* **13**, 11–14.
55 Hubbard SJ & Thornton JM (1993) NACCESS, Computer Program. Department of Biochemistry and Molecular Biology, University College, London, UK.
56 Colombo MF, Rau DC & Parsegian VA (1992) Protein solvation in allosteric regulation: a water effect on hemoglobin. *Science* **256**, 655–659.
57 Shimizu S (2004) Estimating hydration changes upon biomolecular reactions from osmotic stress, high pressure, and preferential hydration experiments. *Proc Natl Acad Sci USA* **101**, 1195–1199.
58 Stagg L, Zhang SQ, Cheung MS & Wittung-Stafshede P (2007) Molecular crowding enhances native structure and stability of alpha/beta protein flavodoxin. *Proc Natl Acad Sci USA* **104**, 18976–18981.
59 Christiansen A & Wittung-Stafshede P (2013) Quantification of excluded volume effects on the folding landscape of Pseudomonas aeruginosa apoazurin *in vitro*. *Biophys J* **105**, 1689–1699.
60 Schurke P, Freeman JC, Dabrowski MJ & Atkins WM (1999) Metal-dependent self-assembly of protein tubes from *Escherichia coli* glutamine synthetase. Cu(2+) EPR studies of the ligation and stoichiometry of intermolecular metal binding sites. *J Biol Chem* **274**, 27963–27968.
61 De Carlo S & Harris JR (2011) Negative staining and cryo-negative staining of macromolecules and viruses for TEM. *Micron* **42**, 117–131.
62 Swerdlow RD, Ebert RF, Lee P, Bonaventura C & Miller KI (1996) Keyhole limpet hemocyanin: structural and functional characterization of two different subunits and multimers. *Comp Biochem Physiol B Biochem Mol Biol* **113**, 537–548.
63 Markl J (2013) Evolution of molluscan hemocyanin structures. *Biochim Biophys Acta* **1834**, 1840–1852.
64 Harris JR, Scheffler D, Gebauer W, Lehnert R & Markl J (2000) *Haliotis tuberculata* hemocyanin (HtH): analysis of oligomeric stability of HtH1 and HtH2, and comparison with keyhole limpet hemocyanin KLH1 and KLH2. *Micron* **31**, 613–622.
65 Phipps BM, Hoffmann A, Stetter KO & Baumeister W (1991) A novel ATPase complex selectively accumulated upon heat shock is a major cellular component of thermophilic archaebacteria. *EMBO J* **10**, 1711–1722.
66 Furutani M, Iida T, Yoshida T & Maruyama T, Group II chaperonin in a thermophilic methanogen, Methanococcus thermolithotrophicus (1998) Chaperone activity and filament-forming ability. *J Biol Chem* **273**, 28399–28407.
67 Gourlay LJ, Bhella D, Kelly SM, Price NC & Lindsay JG (2003) Structure-function analysis of recombinant substrate protein 22 kDa (SP-22). A mitochondrial 2-cys peroxiredoxin organized as a decameric toroid. *J Biol Chem* **278**, 32631–32637.
68 Phillips AJ, Littlejohn J, Yewdall NA, Zhu T, Valéry C, Pearce FG, Mitra AK, Radjainia M & Gerrard JA (2014) Peroxiredoxin is a versatile self-assembling tecton for protein nanotechnology. *Biomacromolecules* **15**, 1871–1881.
69 Harris JR (1969) Some negative contrast staining features of a protein from erythrocyte ghosts. *J Mol Biol* **46**, 329–335.